Liquid Crystals
Publication details, including instructions for authors and subscription information:
http://www.informaworld.com/smpp/title~content=t713926090

Liquid crystal binary mixtures 8CB+8OCB: critical behaviour at the smectic A-nematic transition

M. B. Sied; D. O. López; J. Ll. Tamarit; M. Barrio

Online publication date: 11 November 2010

To cite this Article Sied, M. B. , López, D. O. , Tamarit, J. Ll. and Barrio, M.(2002) 'Liquid crystal binary mixtures 8CB+8OCB: critical behaviour at the smectic A-nematic transition', Liquid Crystals, 29: 1, 57 — 66
To link to this Article: DOI: 10.1080/02678290110093831
URL: http://dx.doi.org/10.1080/02678290110093831

LIQUID CRYSTALS, 2002, VOL. 29, NO. 1, 57–66

Liquid crystal binary mixtures 8CB + 8OCB: critical behaviour at the smectic A–nematic transition

M. B. SIED, D. O. LÓPEZ*, J. Ll. TAMARIT and M. BARRIO

Departament de Física i Enginyeria Nuclear,
E.T.S.E.I.B. Universitat Politècnica de Catalunya, Diagonal 647, 08028 Barcelona,
Catalonia, Spain

(*Received 16 December 2000; accepted 27 June 2001*)

The experimental determination by means of DSC together with a thermodynamic analysis of the two-component phase diagram of octylcyanobiphenyl (8CB)+ octyloxycyanobiphenyl (8OCB) has been performed. The thermodynamic consistency of the two-component system has been proved and similar excess Gibbs energies for mixtures in the isotropic, nematic and smectic phases have been obtained. In order to study the order of the nematic to smectic A phase transition, specific heat measurements obtained using modulated DSC have been made on three mixtures of 8CB+ 8OCB as well as on the pure components. An evolution of the α-critical exponent has been found when the composition of the mixture changes between pure 8CB and pure 8OCB showing crossover behaviour between 3D-XY universal class and the tricritical point. As the 8OCB content in the mixture is further increased, the α-value decreases with the decrease in the McMillan ratio (T_{NA}/T_{NI}) giving rise to a value of about 0.96 at which the 3D-XY mode would be hypothetically reached. The tricritical point would be hypothetically reached at a McMillan ratio of about 0.99 and the extrapolated tricritical amplitude ratio A^-/A^+ is estimated to be 1.6, a value very different from that obtained for the ^{3}He-^{4}He tricritical transition, but comparable with other experimental results reported in the literature.

1. Introduction

Liquid crystal materials are generally composed of molecules which have several common characteristics, such as highly anisotropic structures, strong dipoles or easily polarizable substituents. These materials melt in stages, i.e. there are several intermediate phases (mesophases) between the anisotropic ordered crystal (Cr) and the isotropic liquid (I). Two of the more common mesophases are the orientationally ordered nematic (N) and the layered smectic A (SmA) phases. The N–SmA phase transition has been the most extensively studied of all liquid crystal phase transitions. Thirty years ago, McMillan [1] predicted, by means of the mean-field approximation, that in some cases the N–SmA phase transition could be second order in nature and, essentially simultaneously, de Gennes [2] pointed out the close analogy between the N–SmA transition and the superfluid helium transition. Based on this analogy, de Gennes thought that the N–SmA transition should belong to the 3D-XY universality class ($d = 3$ for the dimensionality of the system and $n = 2$ or XY for the symmetry of the order parameter; the complex order parameter ψ of the SmA phase involves the amplitude and the phase of the density wave). It may be underlined that the general concept of *universality* has allowed the classification of many different phase transitions into universality classes [3]. The mean idea of such a concept implies that the critical exponents describing the critical behaviour of certain macroscopic properties (for example, the specific heat) should only depend on the spatial dimension d, the symmetry n of the order parameter, and the symmetry and range of interactions, but not on the microscopic details of the system.

The critical exponents are influenced by two factors: the strength of the coupling between the smectic order parameter ψ and the nematic orientational order parameter S, and the coupling between the former and the director fluctuations $\delta\mathbf{n}$. The SmA–N transition is influenced by the proximity of the N–I transition, and the pre-asymptotic 3D-XY model is only applicable to systems where the nematic order has completely saturated. So, as a function of the couplings, weaker for a large nematic range, the N–SmA transition is driven away from the 3D-XY behaviour towards tricritical behaviour; the tricritical point is the temperature at which the

* Author for correspondence;
e-mail: david.orencio.lopez@upc.es

Liquid Crystals ISSN 0267-8292 print/ISSN 1366-5855 online © 2002 Taylor & Francis Ltd
http://www.tandf.co.uk/journals
DOI: 10.1080/02678290110093831

change between second order to first order takes place. The intermediate values of the critical exponents are called *effective* or *crossover* exponents and constitute the so-called non-universal exponents. Nowadays, there are basically two mechanisms, by which to modify the strength of the coupling: one involves the confinement of the bulk liquid crystal into porous membranes inducing a decoupling mechanism [4–8] while the second is to change the nematic range. The latter can be achieved, for example, by using binary liquid crystal mixtures [9–15]. Within this framework, the main question is: to what extent does the nematic range give rise to 3D-XY behaviour?

During the last two to three decades, intensive experimental studies have been carried out on the 4-cyano-4-alkylbiphenyls (nCB) (n being the number of carbons in the alkyl chain) and the 4-cyano-4′-alkoxybiphenyls (nOCB) (n has the same meaning as for nCB) series of compounds because of their simple molecular structures as well as their particular polymorphism. Specifically, both series have typical liquid crystalline mesophase sequences depending on the chain lengths. For the nCB series the transitions are Cr–N–I ($n = 5, 6, 7$), Cr–SmA–N–I ($n = 8, 9, 11$) and Cr–SmA–I ($n = 10, 12$); and for the nOCB series Cr–N–I ($n = 5, 6, 7$), Cr–SmA–N–I ($n = 8, 9$) and Cr–SmA–I ($n = 10, 12$). X-ray diffraction studies [16] showed that the mesophases have interdigitated structures with overlapping of core regions due to the strong dipole moment of the CN group. The SmA mesophase, is characterized by smectic layer spacings d, such that $l < d < 2l$, where l denotes the length of the molecule. Thus this smectic phase is referred to as a *partial bilayer smectic* and denoted SmA_d.

From among the members of the nCB and nOCB series with SmA–N transitions, 8CB and 8OCB have been extensively studied during the past twenty years. Here we describe research concerned not only with the pure components but also with their binary mixtures for which the experimental and calculated binary mesogenic two-component system has been stated. Likewise, a study of the order of the SmA–N transition in terms of the specific heat critical exponents has been made, on the pure components and on three binary mixtures covering around five decades of the reduced temperature range.

This paper is organized as follows. In § 2 we describe the experimental details. In § 3 a presentation of the experimenal results concerned with the two-component system 8CB + 8OCB along with a thermodynamic analysis is made. In § 4 a study of the order of the SmA–N transition by means of specific heat data for the pure components and for three mixtures of the two-component system is performed. The results for the critical exponents are compared with others published previously where possible. Likewise, a discussion in the light of 3D-XY-universality class and crossover behaviour is carried out. Finally, in § 5 a summary of the main conclusions is made.

2. Experimental

2.1. *Materials*

The pure components 8CB and 8OCB were synthesized and purified by Prof. Dabrowsky in the Institute of Chemistry, Military University of Technology, Warsaw, Poland. The purity was stated to be higher than 99.9% and no furher purification was made.

Mixtures of 8CB + 8OCB were prepared at room temperature by weighing appropriate amounts of the pure components. To achieve good mixing, samples were sealed in 40 µl aluminium pans and heated to the isotropic phase and then cooled to room temperature.

2.2. *Thermal measurements*

Thermal measurements were performed using a TA Instruments DSC 2920 equipped with modulated DSC and a refrigerating cooling accessory (200 K). The DSC cell was purged with a dry helium flow. In order to obtain the two-component system, standard DSC measurements were made on various selected mixtures and on the pure components. The scanning rates were 2 K min^{-1} and the sample masses were chosen in the range 5–10 mg.

The modulated DSC (MDSC) technique, described in detail elsewhere [17–19], stems from a combination of standard DSC and a.c. calorimetry. The principle of this method is first to subject the sample to a sinusoidal modulated heating rate, and then to process the calorimetric response using a mathematical treatment, namely, to deconvolute the sample's response by means of a discrete Fourier transform method. This technique provides the ability to measure specific heat directly in a single experiment, and to measure it even at very slow underlying heating rates. Although a.c. calorimetry has some advantages when measuring specific heats, other features of its design make is unsuitable for making quantitative measurements of, for example, latent heats of first order transitions. The MDSC experiment is defined by basically three parameters: the frequency or period of modulation, the underlying heating rate and the amplitude of modulation. An evaluation of suitable conditions for the MDSC runs was performed in order to obtain a linear response and steady state throughout the transition. The parameters were chosen to be: a period of 30 s, a modulation amplitude of ± 0.035 K and an underlying heating/cooling rate of 0.01 K min^{-1}. Likewise, the sample mass was selected to ensure a uniform thin layer within the aluminium pan. The specific heat calibration was performed using pure synthetic sapphire, although the absolute accuracy is usually no better than 5% or even worse.

Table 1. Thermal properties of pure 8CB and 8OCB.

	Cr → SmA		SmA → N		N → I		
Compound	T/K	ΔH(kJ mol^{-1})	T/K	ΔH(kJ mol^{-1})	T/K	ΔH(kJ mol^{-1})	Ref.
8CB	294.15	22.19	305.65	—	313.15	—	[24]
	294.20	23.43	306.70	—	313.20	0.61	[25]
	295.15	25.70	306.95	$\leqslant 4\times10^{-4}$	313.95	0.61	[26]
	—	—	307.20	0.14	314.00	0.62	[5]
			306.95	0.27			[6]
	294.46	22.62	306.43	<0.02	313.75	0.63	This work
8OCB	327.65	24.70	340.15	—	353.15	—	[24]
	327.00	24.67	340.00	—	353.00	—	[27]
	—	—	340.4	$<9\times10^{-4}$	—	—	[28]
	—	—	340.27	$<5\times10^{-3}$	353.39	—	[29]
	—	—	340.15	—	354.15	—	[30]
	327.68	26.65	340.37	<0.03	353.39	0.63	This work

3. Two-component system

In this section, a complete determination of the two-component system will be described. In § 3.1, we describe the experimental study using MDSC. It is clear that, although this technique provides an increase in the experimental accessibility of phase diagram data, its use will be at the expense of the reliability and accuracy of the data. To a certain extent, this disadvantage can, however, be overcome by subjecting the experimental data to thermodynamic analysis (§ 3.2), i.e. the internal consistency of the data can be checked and the experimental diagram optimized. In addition, some information about excess properties of the binary mixtures can be obtained.

3.1. *Experimental study*

Both pure components have the same phase sequence (Cr–SmA–N–I), but the polymorphism of 8OCB is slightly more complicated. As pointed out by Hori and Wu [20], 8OCB has four different crystalline phases. Three of them are metastable phases and the structures of two of them were determined to be triclinic and monoclinic [21]. The structure or lattice parameters of the most stable crystalline phase found in commercial samples have not yet been solved. The work by Hori and co-workers to obtain a single crystal of 8OCB was unsuccessful and the powder pattern indicates that the cell is very large and therefore it was not possible to index the pattern [22]. As far as 8CB is concerned, it seems that only one stable crystalline phase exists, the structure of which was recently solved by Kuribayashi and Hori [23] as monoclinic $P2_1/n$ ($Z=4$).

Taking into account the stable phases of both pure components, a brief summary of the available thermal information along with our experimental results is gathered in table 1. For the pure components, the Cr–SmA and N–I transitions are known to be first order and no additional studies have been made concerning this. By contrast, the SmA–N transition is known to be second order and a detailed study of this is made in § 4.

By collating the information obtained from standard DSC measurements, the experimental two-component phase diagram from room temperature to the isotropic state has been determined and is shown in figure 1 (*a*). In the low temperature side of the phase diagram, there exist a eutectoid invariant, or three-phase [Cr_{8CB} + SmA + Cr_{8OCB}] equilibrium at 285.4 K. It is important to realize that the uncertainty in temperature of the invariant increases on increasing the 8OCB content of the mixture. This is a normal effect when the composition of the mixture moves away from the eutectoid composition. This composition and the concentration limits of the invariant temperature have been determined by means of the Tammann diagram (see figure 2). The mole fraction limits are given in table 2. The miscibility in the crystalline phases at room temperature is rather limited, a fact that could be expected taking into account the nature of the molecules and the lattice symmetries (probably non-isostructural phases). Likewise, at higher

Table 2. Experimental (E) and calculated (C) temperatures and mole fraction limits characterizing the three-phase equilibrium for the two-component system.

			Limits		
Invariant		T/K	left	eutectoid	right
Eutectoid	E	285.36	0.05[a]	0.28[a]	0.90[a]
	C	286.70	0.02	0.23	0.97

[a] Data from Tammann diagram in figure 2.

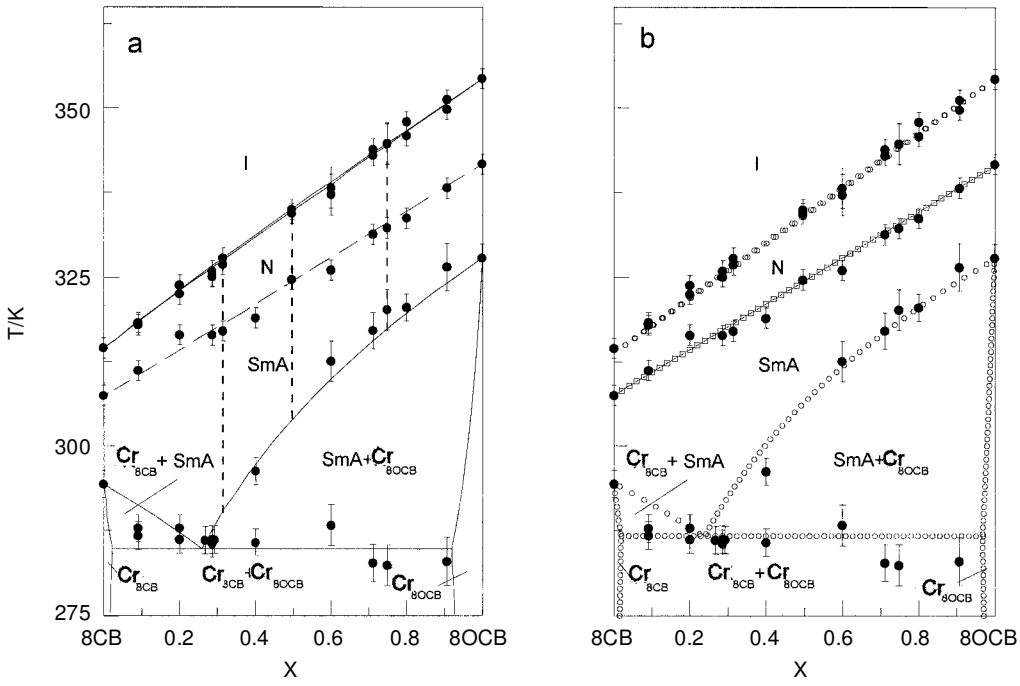

Figure 1. Experimental (*a*) and calculated (*b*) phase diagrams for the two-component system, 8CB+ 8OCB. (□ □) Calculated SmA–N second-order transition line. Dashed vertical lines denote three compositions: X = 0.31, 0.50 and 0.75.

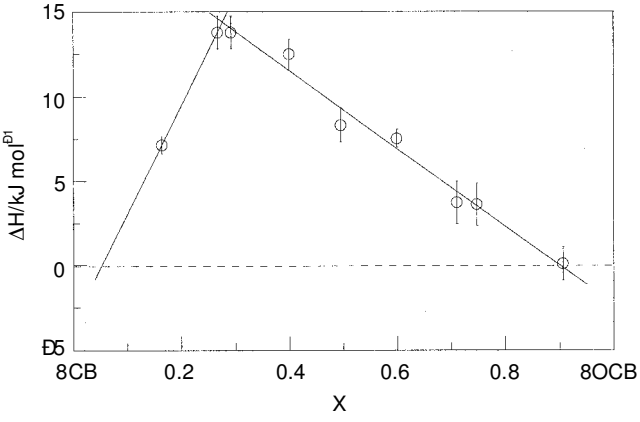

Figure 2. Tammann diagram corresponding to the eutectoid invariant at 285.4 K.

temperatures, we find a continuous evolution with composition for the second order SmA–N transition and a very narrow two-phase equilibrium for the N–I transition.

Three years ago, an experimental phase diagram for mixtures of 8CB+ 8OCB was published by Sharaoui *et al.* [31]. At first glance, the schematic view of the phase diagram has the same main characteristics as shown in figure 1. It is important to note that in their work, different measurements were made. The preparation of the mixtures was done by the contact method and the phase diagram was constructed by means of microscopy.

3.2. *Thermodynamic analysis*

In a thermodynamic analysis of a two-component system A+ B, each stable or metastable form or phase is equivocally associated to a molar Gibbs energy function that contains all thermodynamic information. The equilibrium phase diagram can be constructed when all the possible molar Gibbs functions are known or partially known.

Let us assume a binary mixture between two components A and B in an arbitrary form α. The isobaric Gibbs energy is a temperature- and composition-dependent function that can be written as follows

$$G^{\alpha}(X,T) = (1-X)\mu_{A}^{*,\alpha}(T) + X\mu_{B}^{*,\alpha}(T) + RT[(1-X)\ln(1-X) + X\ln X] + G^{E,\alpha}(X,T) \quad (1)$$

where X represents the mole fraction of the second component B, $\mu_{A}^{*,\alpha}(T)$ and $\mu_{B}^{*,\alpha}(T)$ the Gibbs energies of pure components A and B, respectively; R is the gas constant and $G^{E,\alpha}(T, X)$ is the excess Gibbs energy that accounts for the deviation of the mixture in form α from the ideal mixing behaviour. A knowledge of the above expression for each form is generally unavailable, particularly because $\mu_{A}^{*,\alpha}(T)$, $\mu_{B}^{*,\alpha}(T)$ and $G^{E,\alpha}(T, X)$ are not normally known. However, in order to determine and to analyse a two-phase equilibrium region between two arbitrary forms α and β in a two-component phase

diagram, a simplified treatment, named Equal-Gibbs Curve (EGC) method [32] can be made. In such a way, the difference between the Gibbs energies of α and β forms are zero on the EGC. This occurs for each X at different temperatures, giving rise to a temperature versus composition curve, the so-called EGC-curve, $T_{EGC}(X)$. This curve can be written as:

$$T_{EGC}(X) = \frac{(1-X)\Delta H_A^* + X\Delta H_B^*}{(1-X)\Delta S_A^* + X\Delta S_B^*} + \frac{\Delta G_{EGC}^E(X)}{(1-X)\Delta S_A^* + X\Delta S_B^*}. \quad (2)$$

The first term of the righthand side of equation (2) is only pure-component dependent and can be obtained from pure component data. However, the second term depends on the excess Gibbs energy difference along the EGC-curve. The EGC-method requires some experimental data describing the [α + β] equilibrium to perform an iterative procedure in which one obtains a reasonable EGC and in addition the $\Delta G_{EGC}^E(X)$. This procedure can be automatically done by means of the WINIFIT 2.0-program [33] (based upon MS-DOS LIQFIT and PROPHASE programs [34, 35]) which also allows calculation of the different equilibrium compositions at each temperature, that is to say, the complete binary phase diagram. The program was successfully tested in other thermodynamic analyses for two-component systems [36–39].

The first step in the analysis is to consider the experimental data points for the [N + I] equilibrium. The EGC method via the WINIFIT program provides the excess Gibbs energy difference between the N and I phases along the EGC curve $\Delta G^E(X)$. The result for this difference at the mean temperature $T_m = T_{EGC}(X = 0.5)$ is given by a Redlich–Kister polynomial

$$\Delta G^E(X, T_m) = G^{E,I}(X, T_m) - G^{E,N}(X, T_m) = 10X(1-X)\ \mathrm{J\ mol^{-1}}. \quad (3)$$

Using this approach, we see that the nematic and isotropic phases have practically the same deviation with regard to ideal mixing.

The second order SmA–N transition can also be calculated using WINIFIT by comparing the Gibbs energy curves of the SmA and N phases at each temperature. In this case, there is no phase coexistence region between the SmA and N phases—only a line is drawn in figure 1 (*b*). Similarly, from the thermodynamic analysis of the second order line, we see that both phases, SmA and N, have the same excess Gibbs energy.

The crystalline Cr_{8CB} and Cr_{8OCB} are probably non-isostructural forms. Keeping this fact in mind, the thermodynamic analysis of the Cr + SmA equilibria can be performed using the concept of crossed isodimorphism [36, 39]. This means that the existence of two simple loops crossing each other, gives rise to a eutectoid three-phase equilibrium: one of the loops involves the [Cr_{8CB} + SmA] equilibrium and the other the [Cr_{8OCB} + SmA] equilibrium. An important part of the analysis consists of finding the metastable ends of these loops: the metastable transition points $Cr_{8CB} \rightarrow$ SmA in pure 8OCB and $Cr_{8OCB} \rightarrow$ SmA in pure 8CB. This information, experimentally unknown, must be extracted by extrapolating the known stable parts of these loops. However, the information on stable parts is unfortunately rather limited, particularly for the [Cr_{8CB} + SmA] equilibrium. For this reason, the present analysis attempts to establish a better agreement between the experimental and the calculated phase diagrams. To start with, the metastable transition temperatures of pure 8CB and pure 8OCB were found, via the WINIFIT program, as a result of a great number of trial and error calculations. The chosen values were 200 and 265 K, respectively. Due to the lack of information, the entropy of transition of each metastable crystalline phase was taken to be the same as that of each stable crystalline phase. It should be noted that the results of the analysis remain practically unchanged by slight modifications of the above metastable parameters. The results of such analysis expressed as Redlich–Kister polynomials are

$$G^{E,Cr_{8CB}}(X, T_m) = X(1-X)[4500 - 50(1-2X)]\ \mathrm{J\ mol^{-1}} \quad (4)$$

$$G^{E,Cr_{8OCB}}(X, T_m) = X(1-X)[4500 + 4000(1-2X)]\ \mathrm{J\ mol^{-1}}. \quad (5)$$

The equations (3), (4) and (5) and the metastable data points of the pure components along with the stable data of the pure components listed in table 1 have been used to calculate the complete 8CB + 8OCB phase diagram by means of the WINIFIT program. The phase diagram calculation together with the experimental temperature–composition data are shown in figure 1 (*b*). At first glance, the experimental data are quite well reproduced by this calculation despite the lack of information, especially the unknown metastable properties. A comparison between the calculated and experimental values corresponding to the three-phase equilibrium is given in table 2.

4. SmA–N transition

The study of the order of the SmA–N transition has been performed by measuring the specific heat of the pure components 8CB and 8OCB and of the three mixtures with mole fractions $X = 0.31$, 0.50 and 0.75, see dashed lines in figure 1 (*a*). These measurements of the specific heat variation associated with the SmA–N

transition against $(T - T_{peak})/T_{peak}$ are shown in figure 3. It is important to realize that the absolute value of specific heat data has been corrected and compared with other data previously published. The correction factor was similar for 8CB and 8OCB and has also been applied to the specific heat data of the mixtures. In addition as can be seen in figure 3, the SmA–N transition in the binary mixtures is rounded and broadened as compared with that observed for the pure components.

4.1. *Data analysis and discussion*

The specific heat data shown in figure 3 have been analysed using the renormalization-group expression [40]

$$C_p^{\pm} = B + E\left[\frac{T}{T^{\pm}} - 1\right] + A^{\pm}\left|\frac{T}{T^{\pm}} - 1\right|^{-\alpha}\left[1 + D^{\pm}\left|\frac{T}{T^{\pm}} - 1\right|^{0.5}\right] \quad (6)$$

where $\pm$ indicates above and below the transition. T^+ is the temperature towards which nematic behaviour diverges and T^- is the temperature towards which smectic behaviour diverges. If the transition is first order, then T^- is always greater than T^+. By contrast, if the transition is second order, then $T^- = T^+$ and one refers to a critical temperature T_c $(= T^- = T^+)$ or a peak temperature and $(T - T_c)/T_c$ is the reduced temperature, ε. $A^{\pm}$ are the corresponding amplitudes above and below and the constants B and E account for the specific heat background, the same above and below the transition. α is the specific heat-critical exponent, also the same above and below the transition. The term $D^{\pm}|\varepsilon|^{0.5}$ is the first order correction-to-scaling term, which has been added to the simple power law expression to guarantee the smooth variation of the background at T_c. The exponent of this term is set equal to 0.5, essentially the XY value of 0.524 and no additional fit was tried. The theory for the 3D-XY universality class predicts an amplitude ratio of $(A^-/A^+) = 0.971$ and $D^-/D^+ \approx 1$. Equation (6) is used for pure liquid crystal compounds and can also be used for mixtures of homologous compounds. For the mixtures dealt with in this work, the measurements are at constant mole fraction and it seems physically reasonable that no appreciable distinction exists with the measurements performed at constant chemical potential difference.

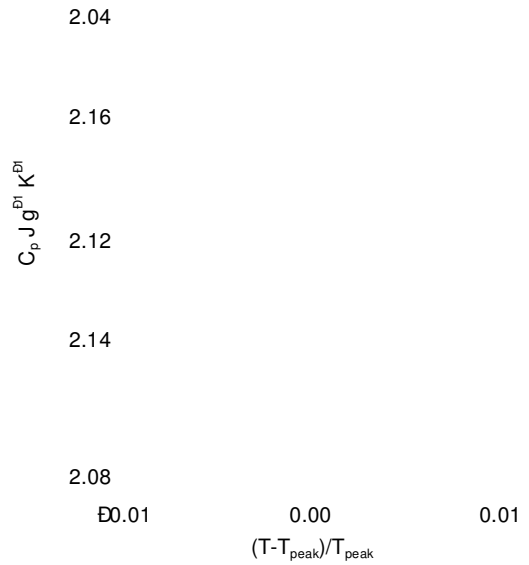

Figure 3. Specific heat as a function of $(T - T_{peak})/T_{peak}$ near the SmA–N transition in pure 8CB and 8OCB and in three mixtures of 8CB + 8OCB.

Table 3 lists the values of the critical exponent α, the amplitude ratio A^-/A^+, the first correction to the scaling ratio D^-/D^+ and the critical temperature over different ranges of the reduced temperature (ε), using equation (6) for the pure components and for the three mixtures. It should be noted that the results for the pure components are given for three different reduced temperature ranges in order to evaluate the dependence of the adjustable parameters on the variation of the temperature range. As we can see, the value of α is rather insensitive to the change of the temperature range. The physical meaning of the values of the correction-term amplitudes (D^- and D^+) is not clear because of the change in sign. The ratio D^-/D^+ reaches a stable value for 8CB and changes significantly for 8OCB on changing the fitted range. By contrast, a stable amplitude ratio A^-/A^+ is obtained for both pure components. A preliminary fit of T^+ and T^- showed a difference between them smaller than the uncertainty in temperature. In this basis $T^+ = T^- = T_c$ as used as a unique parameter in the fit of equation (6). As for the three mixtures, the results listed in table 3 represent well the measured C_p data as indicated by the χ^2 values. In order to compare the data, the same maximum reduced temperature was considered in all the fits. The minimum reduced temperature was slightly different for each mixture owing to the existence of rounding-off in the specific heat data near the maximum of the peak.

In table 4 we have summarized the available experimental information on the pure components 8CB and 8OCB. For 8CB, there is quite good agreement between our value of α and other experimental values which

Table 3. Results of fits to equation (6) for pure 8CB and 8OCB and three mixtures. The minimum value of ε is 7×10^{-5} for pure 8CB and 10^{-5} for pure 8OCB while it is $\approx 2\times10^{-5}$ for the mixtures. N is the number of data points included in these fits. The errors quoted are the statistical uncertainties.

X_{8OCB}	$\lvert\varepsilon\rvert_{max}$	N	α^{b}	A^-/A^+	D^-/D^+	T_c/K	χ^2
0(8CB)	$\leqslant 5\times10^{-3}$	350	0.32 ± 0.01	1.09 ± 0.09	1.7 ± 0.2	306.433 ± 0.005	2×10^{-3}
	$\leqslant 2\times10^{-3}$	140	0.31 ± 0.01	1.2 ± 0.1	$1.7+0.3$	(306.433)[a]	10^{-3}
	$\leqslant 10^{-3}$	70	0.31 ± 0.02	1.16 ± 0.07	$1.6+0.9$	(306.433)[a]	2×10^{-3}
0.31	$\leqslant 2\times10^{-3}$	98	0.20 ± 0.06	1.1 ± 0.5	0.6 ± 0.6	313.65 ± 0.02	10^{-2}
0.50	$\leqslant 2\times10^{-3}$	78	0.14 ± 0.04	1.37 ± 0.03	0.16 ± 0.04	324.49 ± 0.02	6×10^{-3}
0.76	$\leqslant 2\times10^{-3}$	71	0.09 ± 0.03	0.86 ± 0.07	1.0 ± 0.1	333.40 ± 0.02	10^{-3}
1(8OCB)	$\leqslant 5\times10^{-3}$	286	0.044 ± 0.002	1.01 ± 0.01	0.6 ± 0.2	340.37 ± 0.01	10^{-3}
	$\leqslant 2\times10^{-3}$	110	0.044 ± 0.002	1.01 ± 0.02	$0.9+1.0$	(340.37)[a]	2×10^{-3}
	$\leqslant 10^{-3}$	62	0.044 ± 0.003	1.01 ± 0.05	$1.4+6.2$	(340.37)[a]	10^{-3}

[a] Values in parentheses indicate that the parameter was held constant at the quoted value.
[b] The value was fitted with the constraint $\alpha^+ = \alpha^-$.

Table 4. Comparison between selected parameter values (α, A^-/A^+, D^-/D^+ and T_c) reported from different literature sources for the SmA–N transition for the pure compounds 8CB and 8OCB

Compound	$\lvert\varepsilon\rvert_{min}$—$\lvert\varepsilon\rvert_{max}$	α	A^-/A^+	D^-/D^-	T_c/K	Ref.
8CB	—	0.30 ± 0.05	1.08	—	306.690	[41]
	10^{-4}—2.5×10^{-3}	0.285 ± 0.03	1.03	—	307.017 ± 0.012	[42]
	10^{-6}—2×10^{-3}	0.31 ± 0.03	0.83 ± 0.05	-2.6	306.9216 ± 0.0003	[26]
	5×10^{-5}—10^{-2}	0.26 ± 0.01	1.08 ± 0.07	0.76 ± 0.08	307.0140 ± 0.0002	[4]
	7×10^{-5}–2×10^{-3}	0.31 ± 0.01	1.2 ± 0.1	1.7 ± 0.3	306.433 ± 0.005	This work
8OCB	3×10^{-5}–3×10^{-3}	0.20 ± 0.05	1.016	—	340.267	[29]
	6×10^{-5}—5×10^{-3}	0.025 ± 0.04	0.72	—	340.108 ± 0.003	[42, 43]
	2.5×10^{-5}–1.26×10^{-3}	0.25 ± 0.02	0.83	—	340.193 ± 0.002	[42]
	4×10^{-5}—3×10^{-3}	0.175 ± 0.03[a]	2.96[a]	—	340.403 ± 0.002[b]	[28]
	10^{-5}—5×10^{-3}	0.044 ± 0.002	1.01 ± 0.01	0.6 ± 0.2	340.37 ± 0.01	This work

[a] These results are questioned by the authors. Other possibilities give $\alpha = -0.014$ and $A^-/A^+ = 0.74$.
[b] This temperature is the average value between T^+ and T^-.

range between 0.26 and 0.31. As for the ratio A^-/A^+, our value is above unity, and comparable to other experimental values, with the exception of the value reported by Thoen and co-workers which is slightly lower than 0.971 (the theoretical value for 3D-XY universality class). As far as 8OCB is concerned, there exist considerable discrepancies between the published experimental results. Our result for α is in very good agreement with the value reported by LeGrange and Mochel [42, 43] and equivalent to that proposed by Johnson *et al.* [44] for which α can be -0.014 and $A^-/A^+ = 0.74$ (see table 4; another possibility is $\alpha = 0.175$ and $A^-/A^+ = 2.96$). Garland's value [29] and even another measurement made by LeGrange and Mochel on a sample of the same batch is around 0.20, so considerably different from our result. LeGrange and Mochel suggested that very small but differing concentrations of impurities are responsible for the dual behaviour of 8OCB.

From equation (6), we can define the parameter μ as follows

$$\mu = \frac{C_p^{\pm} - B - E\varepsilon}{1 + D^{\pm}\lvert\varepsilon\rvert^{0.5}} = A^{\pm}\lvert\varepsilon\rvert^{-\alpha}. \qquad (7)$$

Thus in a double logarithmic plot a linear relationship, with slope $-\alpha$, is found between the parameter μ and ε. In figure 4 we show these plots for pure 8CB, 8OCB and the three analysed mixtures. We clearly observe a decreasing of the effective α values from 8CB to 8OCB. It should be noted that there are two sets of data points for each compound and mixture. The displacement corresponds to the different amplitude A above and below the transition. It is important to realize for 8OCB that the two sets of data points are practically coincident ($A^- \approx A^+$). The absence of rounding-off near to 10^{-5} in reduced temperature for this compound should also be noted.

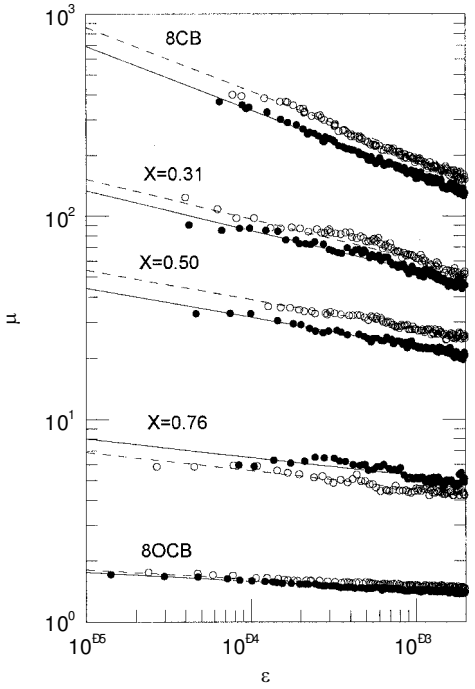

Figure 4. Doubly logarithmic plot for the parameter μ versus reduced temperature ε for pure 8CB and 8OCB and three mixtures between them for N(●) and SmA(○) phases. Solid and dashed lines correspond to the fit using equation (7).

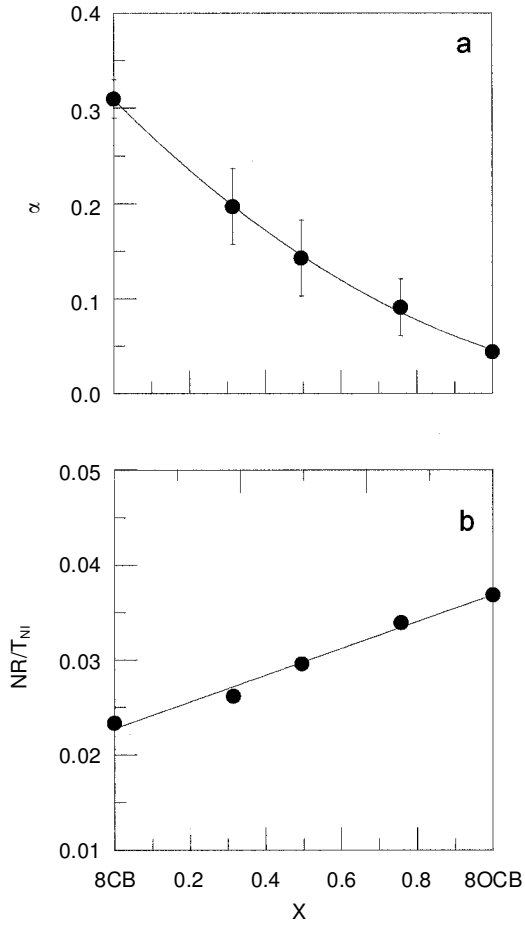

Figure 5. (*a*) Effective critical exponent α versus composition; (*b*) the nematic range normalized by the temperature T_{NI} (NR/T_{NI}) against composition.

Figure 5 (*a*) clearly shows the variation of the effective α values with composition. In figure 5 (*b*), the nematic range NR ($= T_{NI} - T_{AN}$, where T_{NI} is the temperature at which the nematic to isotropic transition occurs and T_{AN} is the corresponding temperature for the SmA to nematic transition) normalized by T_{NI}, is also shown against composition. In fact, NR/T_{NI} is $1-(T_{AN}/T_{NI})$ where T_{AN}/T_{NI} is the McMillan ratio, a measure of the deviation from isotropic 3D-XY behaviour.

An inspection of figures 5 (*a*) and 5 (*b*) suggests a correlation between the effective α values and the McMillan ratio or NR/T_{NI}. In figure 6 (*a*), the α values are plotted against the normalized nematic range. From this we can observe that the extrapolation of the line of best fit at $NR/T_{NI} \approx 0.04$ (or McMillan ratio $T_{AN}/_{NI}$ of about 0.96) reaches the universal 3D-XY α value. In figure 6 (*b*), the ratio A^-/A^+ for pure components and mixtures is also plotted against NR/T_{NI}. In spite of the scatter in the data points, the A^- and A^+ data have large uncertainties; one can observe practically the same value for NR/T_{NI} when the 3D-XY A^-/A^+ value is reached. That is to say, it seems that 3D-XY predictions take place for $NR/T_{NI} \geqslant 0.04$ (or $T_{AN}/T_{NI} \leqslant 0.96$). When the nematic range becomes short ($NR/T_{NI} \leqslant 0.04$), the expected crossover to tricritical behaviour is observed. Although the crossover curve of effective α vs. NR/T_{NI} is not universal, we would expect to find a very similar curve for the data of homologous series. The expected T_{AN}/T_{NI} value at the tricritical point seems to not be universal but probably we could obtain the same value for homologous series. The extrapolation of figure 6 (*a*) at $\alpha = 0.5$ provides a value of NR/T_{NI} of about 0.01, i.e. 0.99 in terms of McMillan ratio. The value of the amplitude ratio A^-/A^+ at 0.01 in NR/T_{NI}, see figure 6 (*b*), gives a value of about 1.6. Despite the arbitrariness of such an extrapolation for the tricritical amplitude ratio, similar experimental values have been observed in other non-homologous and homologous series of compounds [9, 26, 44, 45]. The value of the tricritical amplitude ratio for ^{3}He-^{4}He is about 7, clearly far away from our extrapolated value and other experimental values.

Finally, in order to confirm the above assumptions, studies on binary mixtures between other nCB and nOCB liquid crystals have been undertaken for us.

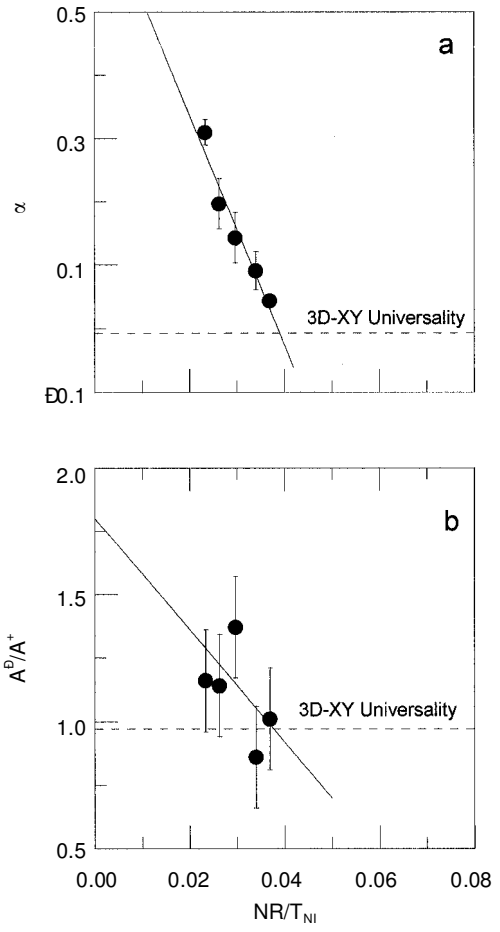

Figure 6. (*a*) Effective critical exponent α versus NR/T_{NI}; (*b*) the amplitude ratio A^-/A^* versus NR/T_{NI}. The dashed line indicates the universal values for the isotropic 3D-XY model.

5. Conclusions

The experimental two-component phase diagram for 8CB + 8OCB has been established by means of DSC. The experimental results have been used in a thermodynamic analysis in which the thermodynamic consistency of the experimental binary phase diagram has been proved. We note also the similarity of the isotropic, nematic and smectic phases from a thermodynamic point of view.

As for the SmA–N transition, it has been shown that this transition is second order in nature, not only for the pure components but also for their mixtures. There exist effective critical exponents α showing crossover behaviour between the 3D-XY model and the tricritical point. In fact there exists a more or less common trend when the effective α and amplitude ratio A^-/A^+ are plotted against NR/T_{NI}. The trend which is represented by a straight line, and is clearer in the plot of α vs. NR/T_{NI} than for the plot of A^-/A^+ vs. NR/T_{NI}, seems to suggest a constant value of NR/T_{NI} for these homologous series of compounds at which the 3D-XY model would be reached. This value is about 0.04, i.e. 0.96 in terms of the McMillan ratio T_{AN}/T_{NI}. In contrast, the tricritical behaviour would seem to be reached at about 0.99 in terms of the McMillan ratio, with an amplitude ratio A^-/A^+ of about 1.6.

The authors are grateful to the DGE for financial support (grant PB98-0932).

References

[1] McMillan, W. L., 1971, *Phys. Rev. A*, **4,** 1238.
[2] De Gennes, P. G., 1972, *Solid State Commun.*, **10,** 753.
[3] Fisher, M. E., 1983, *Scaling, Universality and Renormalization Group Theory* (New York: Springer-Verlag).
[4] Iannacchione, G. S., and Finotello, D., 1994, *Phys. Rev. E*, **50,** 4780.
[5] Quian, S., Iannacchione, G. S., and Finotello, D., 1994, *Phys. Rev. E*, **50,** 4305.
[6] Quian, S., Iannacchione, G. S., and Finotello, D., 1996, *Phys. Rev. E*, **53,** R4291.
[7] Quian, S., Iannacchione, G. S., and Finotello, D., 1997, *Mol. Cryst. liq. Cryst.*, **292,** 175.
[8] Quian, S., Iannacchione, G. S., and Finotello, D., 1998, *Phys. Rev. E*, **57,** 4305.
[9] Thoen, J., Marynissen, H., and van Dael, W., 1984, *Phys. Rev. Lett.*, **52,** 204.
[10] Kortan, A. R., von Kanel, H., Birgeneau, R. J., and Litster, J. D., 1984, *J. Physique*, **45,** 529.
[11] Ocko, B. M., Birgenau, R. J., and Litster, J. D., 1986, *Z. Phys. B*, **62,** 487.
[12] Stine, K. J., and Garland, C. W., 1989, *Phys. Rev. A*, **39,** 1482.
[13] Stine, K. J., and Garland, C. W., 1989, *Phys. Rev. A*, **39,** 3148.
[14] Garland, C. W., Nounesis, G., and Stine, K. J., 1989, *Phys. Rev. A*, **39,** 4919.
[15] Nounesis, G., and Garland, C. W., 1991, *Phys. Rev. A*, **43,** 1849.
[16] Iwakabe, Y., Hara, M., Kondo, K., Toguchi, K., Mukoh, A., Garito, F., Sasabe, H., and Yamada, A., 1990, *Jpn. J. appl. Phys.*, **29,** L22.
[17] Wunderlich, B., Boller, A., Okazaki, I., and Kreitmeier, S., 1996, *Thermochim. Acta*, **282/283,** 143.
[18] Hatta, I., Ichikawa, H., and Todoki, M., 1995, *Thermochim. Acta*, **267,** 83.
[19] Schick, C., Jonsson, U., Vassiliev, T., Minakov, A., Schawe, J., Sherrenberg, R., and Lorinczy, D., 2000, *Thermochim. Acta*, **347,** 53.
[20] Hori, K., and Wu, H., 1999, *Liq. Cryst.*, **26,** 37.
[21] Hori, K., Kurosaki, M., Wu, H., and Itoh, K., 1996, *Acta Cryst.*, **C52,** 1751.
[22] Hori, K., 2000, personal communication.
[23] Kuribayashi, M., and Hori, K., 1998, *Acta Cryst.*, **C54,** 1475.
[24] Hulme, D. S., Raynes, E. P., and Harrison, K. J., 1974, *J. chem. Soc. chem. Comm.*, 98.
[25] Urban, S., and Wurflinger, A., 1997, *Adv. Chem. Phys.*, **98,** 143.

[26] Thoen, J., Marynissen, H., and van Dael, W., 1982, *Phys. Rev. A*, **26,** 2886.
[27] Product information, E. Merck, Germany.
[28] Johnson, D. L., Hayes, C. F., deHoff, R. J., and Shantz, C. A., 1978, *Phys. Rev. B*, **18,** 4902.
[29] Kasting, G. B., Lushington, K. J., and Garland, C. W., 1980, *Phys. Rev. B*, **22,** 321.
[30] Shashidar, R., Ter Minassian, L., Ratwa, B. R., and Kalkura, A. N., 1982, *J. Physique Lett.*, **43,** L239.
[31] Sahraoui, A. H., Kolinsky, C., Delenclos, S., Daoudi, A., and Buisine, J. M., 1997, *J. appl. Phys.*, **82,** 6209.
[32] Oonk, H. A. J., 1981, *Phase Theory. The Thermodynamics of Heterogeneous Equilibria* (Amsterdam: Elsevier).
[33] Daranas, D., Lòpez, R., and Lòpez, D. O., 2000, WINIFIT 2.0 Computer Program, Polytecnical University of Catalonia, Barcelona.
[34] Jacobs, M. H. G., and Oonk, H. A. J., 1990, *LIQFIT: A computer program for the thermodynamic assessment of T–X liquidus or solidus data*, Utrecht University.
[35] Van Duijneveldt, J. S., Baas, F. A. S., and Oonk, H. A. J., 1988, *PROPHASE: An MS-DOS program for the calculation of binary T–X phase diagrams*, Utrecht University.
[36] Salud, J., Lòpez, D. O., Barrio, M., Tamarit, J. L. I., and Oonk, H. A. J., 1999, *J. Mater. Chem.*, **9,** 917.
[37] Pardo, L. C., Barrio, M., Tamarit, J. L. I., Lòpez, D. O., Salud, J., Negrier, P., and Mondieig, D., 1999, *Chem. Phys. Lett.*, **308,** 204.
[38] Lòpez, D. O., Salud, J., Tamarit, J. L. I., Barrio, M., and Oonk, H. A. J., 2000, *Chem. Mater.*, **12,** 1108.
[39] Salud, J., Lòpez, D. O., Tamarit, J. L. I., Barrio, M., Jacobs, M. H. G., and Oonk, H. A. J., 2000, *J. solid state Chem.*, **154,** 390.
[40] Kumar, S., 2001, *Liquid Crystals: Experimental Study of Physical Properties and Phase Transitions* (Cambridge: Cambridge University Press).
[41] Kasting, G. B., Garland, C. W., and Lushington, K. J., 1980, *J. Phys. (Paris)*, **41,** 879.
[42] Legrange, J. D., and Mochel, J. M., 1981, *Phys. Rev. A*, **23,** 3215.
[43] LeGrange, J. D., and Mochel, J. M., 1980, *Phys. Rev. Lett.*, **15,** 35.
[44] Stine, K. J., and Garland, G. W., 1989, *Phys. Rev. B*, **39,** 3148.
[45] Huster, M. E., Stine, K. J., and Garland, C. W., 1987, *Phys. Rev. A*, **36,** 2364.